

Generalized Irwin plastic zone correction of a sub-interface Zener-Stroh crack in a coating-substrate system

J. Zhuang, and *Z. M. Xiao

School of Mechanical and Aerospace Engineering

Nanyang Technological University, Singapore

*Corresponding author: mzxiao@ntu.edu.sg

Abstract

Elastic-plastic stress analysis of a Zener-Stroh crack paralleling to the interface of a coating-substrate system has been carried out in this work. The sum of the Burgers vectors of the climb and the glide dislocations along the crack line account for the stress field around its blunt tip where dislocation enters, and the sharp tip where crack propagates. Firstly, Gauss-Chebyshev quadrature technique is applied to solve the governing equation of dislocation density functions constrained by load-free crack faces. When taking plasticity into account at both crack tips where stresses are high, the generalized Irwin plastic zone correction is recommended. Plastic zone size (PZS) for both tips and crack tip opening displacement (CTOD) for the sharp tip are then obtained. The effects of coating thickness, crack depth, material mismatch and displacement loads ratio onto PZSs and CTOD have been analyzed in detail.

Keywords: Zener-Stroh crack, bi-material coating-substrate composite, singular integral equations, Gauss-Chebyshev quadrature technique, PZS, CTOD.

Introduction

Apart from the well-known Griffith crack, there is another mechanism of cracking as a result of edge dislocations in solids, firstly realized by Zener and Stroh [Stroh (1954); Zener (1948)] in literature. They proposed that the edge dislocations of a pile-up that are stopped at an obstacle, such as a grain boundary (GB), could coalesce into a crack nucleus (Fig. 1). Some situations in which massive Zener-Stroh cracks are coalesced have been recognized: Noticing solids with smaller grain size will possess more GBs, as well as less amount of possible pile up of dislocations at each boundary. More GBs lead to frequent occurrences of dislocation pile-up and more potential sources of crack nucleuses; while less pile up of dislocations accumulated at each location make it harder for dislocations to be repelled and overcome the energetic barrier for diffusion across a GB. That's why GBs are major sinks of dislocations as well. Therefore, knowing more about Zener-Stroh cracks' behaviors in micro- or nano-scale structures is of much significance.

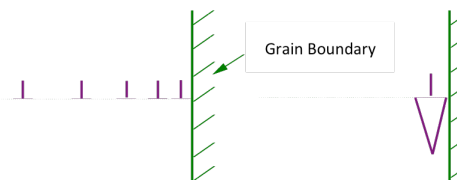


Figure 1. Zener-Stroh crack initiation

Many attractive features of nanocrystalline (nc) and microcrystalline (mc) metals, such as high strength and hardness, and improved resistance to wear and corrosion damage compared to conventional metals have been fully discovered by researchers [Kumar et al. (2003); Zhang et al. (2005)]. However, due to the presence of high-density ensembles of GBs as stoppers for lattice dislocations, nc becomes quite easy

to break, especially those super-refined into ultrasmall grain sizes [Pozdnyakov (2003)]. High stress concentration at GBs will facilitate crack nucleation and growing process, degrading the fracture toughness of the material. Moreover, bulk nanostructured materials usually have disappointingly low ductility. They exhibit a very low uniform elongation due to low work-hardening rate. Localized deformation (necking) under tensile stress often occurs very abruptly because of nc's low dislocation accumulation capability [Zhao et al. (2006)]. In order to enhance both toughness and ductility of nc and mc, without sacrificing their high yield strengths, numerous methodologies and techniques have been suggested [Kuntz et al. (2004); Wang et al. (2002)]. No matter how different they look like, people do believe that fabrication of micro- or nano-composites is the best solution up to now in fulfilling practical needs where both strength and toughness are highlighted.

Although literatures commence to study on the effects of nanocomposites onto fracture toughness as a whole body, the localized behavior, such as how certain types of microcrack are initiated and propagating through the composite is lack of information, especially with plastic zone correction at crack tips. Therefore we manage to start with the investigation of a Zener-Stroh crack lying in a semi-infinite substrate covered by a coating with finite thickness, and check around its crack tips to see how certain properties are improved from single-phase structures. To our best knowledge, most of the time, ductility of nanocomposites, though enhanced, still remains limited compared to their corresponding values of traditional coarse-grained materials. That's why for most cases, the size of the process zone and the plastic region around the crack tip is sufficiently small, so the small-scale yielding assumption is applicable to account for crack tip plasticity [Koch (2007)]. With the additional concern of more complicated configuration and stress field, we proposed a generalized Irwin model in dealing with mode I and mode II stress intensity factors simultaneously. The advantage of this model is that the model itself is intuitive and the procedure can be easily adopted by engineers. Results include the plastic zone size, the crack tip opening displacement, and effective stress intensity factors of mode I and mode II in different scenarios.

The generalized Irwin model of a sub-interface Zener-Stroh crack

The plastic zone size

Current physical problem is depicted in Fig. 2a. Stress fields ahead of the crack tips along x axis can be expressed as [Anderson (2005)]

$$\sigma_{xx}^{(t_m)} = \sigma_{yy}^{(t_m)} = \frac{K_I^{(t_m)}}{\sqrt{2\pi r}}, \sigma_{xy}^{(t_m)} = \frac{K_{II}^{(t_m)}}{\sqrt{2\pi r}}, \sigma_{zz}^{(t_m)} = \nu_2 (\sigma_{xx}^{(t_m)} + \sigma_{yy}^{(t_m)}) = \begin{cases} 0 & \text{Plane stress} \\ \frac{2\nu_2 K_I^{(t_m)}}{\sqrt{2\pi r}} & \text{Plane strain} \end{cases}, m = 1, 2. \quad (1)$$

Here (t_1) , (t_2) stands for the blunt and sharp crack tips, respectively. The subscript 2 refers to the substrate material. ν_2 represents its Poisson's ratio. Due to the Von Mises yield criterion, yielding will occur if the equivalent stress σ_e reaches the yielding stress of material 2, σ_{ys}

$$\sigma_e^{(t_m)} = \sqrt{\frac{(\sigma_{xx}^{(t_m)} - \sigma_{yy}^{(t_m)})^2 + (\sigma_{xx}^{(t_m)} - \sigma_{zz}^{(t_m)})^2 + (\sigma_{zz}^{(t_m)} - \sigma_{yy}^{(t_m)})^2 + 6(\sigma_{xy}^{(t_m)})^2}{2}} = \sigma_{ys} = \frac{K_e^{(t_m)}}{\sqrt{2\pi r}}. \quad (2)$$

The equivalent stress intensity factors K_e are then obtained by

$$K_e^{(t_m)} = \begin{cases} \sqrt{(K_I^{(t_m)})^2 + 3(K_{II}^{(t_m)})^2} & \text{Plane stress} \\ \sqrt{(1-2\nu_2)^2 (K_I^{(t_m)})^2 + 3(K_{II}^{(t_m)})^2} & \text{Plane strain} \end{cases}. \quad (3)$$

From Eq. (2), the first order estimation of PZS can be expressed with respect to σ_{ys} ,

$$r_y^{(t_m)} = \frac{(K_e^{(t_m)})^2}{2\pi\sigma_{ys}^2}. \quad (4)$$

Due to stress relaxation around crack tips, it is clear that the actual plastic strain will be extended to a larger zone. See from Fig. 2b, the 2nd order estimation of PZS, known as plastic zone correction, has the following form:

$$r_p^{(t_m)} = \frac{(K_e^{(t_m)})^2}{\pi\sigma_{ys}^2}. \quad (5)$$

Crack tip opening displacement

The crack tip opening displacement of a Zener-Stroh crack under the generalized Irwin model is shown in Fig. 2c. Although we can see faces are completely open throughout the crack, propagation will be initiated only at the sharp tip due to the existence of tensile stress, not at the blunt tip that has been compressed and stabilized. As a result, only CTOD at the sharp tip will be discussed hereafter. CTOD at the sharp tip δ is given in literature as [Anderson (2005)]

$$\delta = \frac{\kappa_2 + 1}{\mu_2} K_I \sqrt{\frac{r_y^{t_2}}{2\pi}}, \quad (6)$$

μ_2 is the shear modulus. $\kappa_2 = \frac{3-\nu_2}{1+\nu_2}$ for plane stress, and $\kappa_2 = 3-4\nu_2$ for plane strain. Substitute Eq. (4) into (6), with the universal relation $E_2/2\mu_2 = 1+\nu_2$, we have

$$\delta = \frac{4}{\pi E_2'} \cdot \frac{K_I^{t_2} K_e^{t_2}}{\sigma_{ys}}, \quad (7)$$

in which $E_2' = E_2$ for plane stress, $E_2' = \frac{E_2}{1-\nu_2}$ for plane strain. E_2 is the elastic modulus of the substrate.

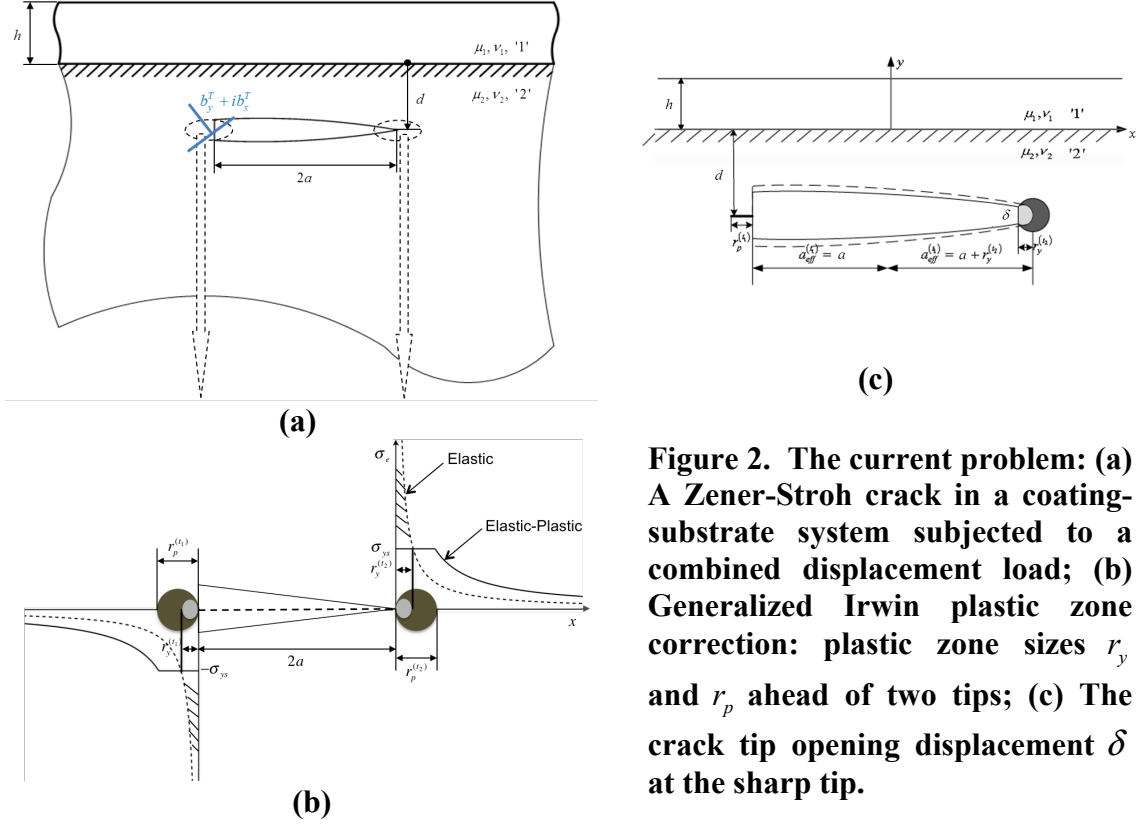


Figure 2. The current problem: (a) A Zener-Stroh crack in a coating-substrate system subjected to a combined displacement load; (b) Generalized Irwin plastic zone correction: plastic zone sizes r_y and r_p ahead of two tips; (c) The crack tip opening displacement δ at the sharp tip.

The effective stress intensity factor

Let's begin with the Zener-Stroh crack of length $2a$ without plastic zone correction. Concentrated climb and glide edge dislocations at the blunt tip would lead to an array of dislocations emitted along the crack line. Due to traction free condition on the crack faces, governing equation of combined distributed dislocation density $B(\xi)$ turns out to be

$$\sigma_{yy}(x) + i\sigma_{xy}(x) = 2 \int_{-a}^a \frac{\overline{B}(\xi)}{x-\xi} d\xi + \int_{-a}^a B(\xi) F_1(x-\xi) d\xi + \int_{-a}^a \overline{B}(\xi) F_2(x-\xi) d\xi = 0, \quad |x| < a \quad (8)$$

where $\overline{(\quad)}$ denotes the complex conjugate. The kernels $F_1(x-\xi)$ and $F_2(x-\xi)$ are given in the literature [Lu and Lardner (1992)]. The boundary conditions are

$$\int_{-a}^a B_x(\xi) d\xi = \frac{\mu_2}{\pi(1+\kappa_2)} b_x^T, \quad \int_{-a}^a B_y(\xi) d\xi = \frac{\mu_2}{\pi(1+\kappa_2)} b_y^T, \quad (9)$$

in which $B_x(\xi)$ and $B_y(\xi)$ are the glide and climb dislocation densities, respectively. b_x^T and b_y^T are the corresponding total sum of Burgers vector in the x and y directions.

Since the dislocation density tends to go infinity in a square root singular manner, B_x and B_y can be rewritten into $B_x(s) = \frac{1}{\sqrt{1-s^2}}\phi_x(s)$ and $B_y(s) = \frac{1}{\sqrt{1-s^2}}\phi_y(s)$, where $\phi_x(s)$ and $\phi_y(s)$ are unknown regular functions. Substituting B_x and B_y into Eqs. (8) and (9), four singular integral equations with Cauchy kernels are obtained. Gauss-Chebyshev quadrature technique is then implemented to solve them numerically, thus B_x and B_y can be obtained [Zhuang et al. (2013)]. Mode I and mode II stress intensity factors at each crack tip can be derived in the following form [Weertman (1996)]

$$\begin{aligned} K_I^{(t_1)} &= -2\pi\sqrt{\pi a}\phi_y(-1), & K_I^{(t_2)} &= 2\pi\sqrt{\pi a}\phi_y(+1), \\ K_{II}^{(t_1)} &= -2\pi\sqrt{\pi a}\phi_x(-1), & K_{II}^{(t_2)} &= 2\pi\sqrt{\pi a}\phi_x(+1). \end{aligned} \quad (10)$$

Here $\phi_x(\pm 1)$ and $\phi_y(\pm 1)$ are values of regular functions at blunt (-1) and sharp (+1) crack tips after the half-crack length a has been normalized to 1.

When we improve our analysis to investigate the elastic-plastic fracture behaviors of the Zener-Stroh crack, plastic zone correction needs to be imposed at both crack tips. The elongated, effective half-crack length is given

$$a_{eff}^{(t_m)} = a + r_y^{(t_m)} = a + \frac{(K_e^{(t_m)})^2}{2\pi\sigma_{ys}^2}. \quad (11)$$

Remember that a Zener-Stroh crack can only propagate from the sharp tip, let's focus on investigation of effective stress intensity factors at that tip. Hence, we get

$$K_I^{eff} = 2\pi\sqrt{\pi a_{eff}^{(t_2)}}\phi_y'(+1), \quad K_{II}^{eff} = 2\pi\sqrt{\pi a_{eff}^{(t_2)}}\phi_x'(+1), \quad (12)$$

where $\phi_x'(+1)$ and $\phi_y'(+1)$ are values of regular functions at the sharp tip after the effective half-crack length $a_{eff}^{(t_2)}$ has been normalized to 1.

Numerical examples and discussion

Some numerical examples and discussions for the plastic zone size, the crack tip opening displacement and effective stress intensity factors of a Zener-Stroh crack of length $2a$ are given. The crack is embedded in a coating-substrate without external loading. The total sum of the Burgers vector throughout the crack $b_y^T + ib_x^T$ ensures faces are fully open. For the ease of assessment, PZS and CTOD are normalized by:

$$\begin{aligned} K_I^0 &= \frac{2\mu_2 b_y^T}{(1+\kappa_2)\sqrt{\pi a}}, & K_{II}^0 &= \frac{2\mu_2 b_x^T}{(1+\kappa_2)\sqrt{\pi a}}, & K_e^0 &= \begin{cases} \sqrt{(K_I^0)^2 + 3(K_{II}^0)^2} & \text{Plane stress} \\ \sqrt{(1-2\nu_2)^2 (K_I^0)^2 + 3(K_{II}^0)^2} & \text{Plane strain} \end{cases} \\ r_0 &= \frac{(K_e^0)^2}{\pi\sigma_{ys}^2}, & \delta_0 &= \frac{4K_I^0 K_e^0}{\pi E_2' \sigma_{ys}}, \end{aligned} \quad (13)$$

where K_I^0 , K_{II}^0 , K_e^0 , r_0 and δ_0 are the mode I, mode II, equivalent stress intensity factors, PZS and CTOD respectively for the same Zener crack that is embedded in a homogeneous infinite plate of material ‘2’. The dependence of the normalized plastic zone size $r_p^{(t_m)}/r_0$, normalized crack tip opening displacement δ/δ_0 , and normalized effective stress intensity factors $K_I^{eff}/K_I^{(t_2)}$ and $K_{II}^{eff}/K_{II}^{(t_2)}$ on the normalized coating thickness h/a , normalized crack depth d/a , the Dundurs’ parameter α , as well as displacement loads ratio b_x^T/b_y^T are shown in Tables 1-2.

Normalized PZS and normalized CTOD

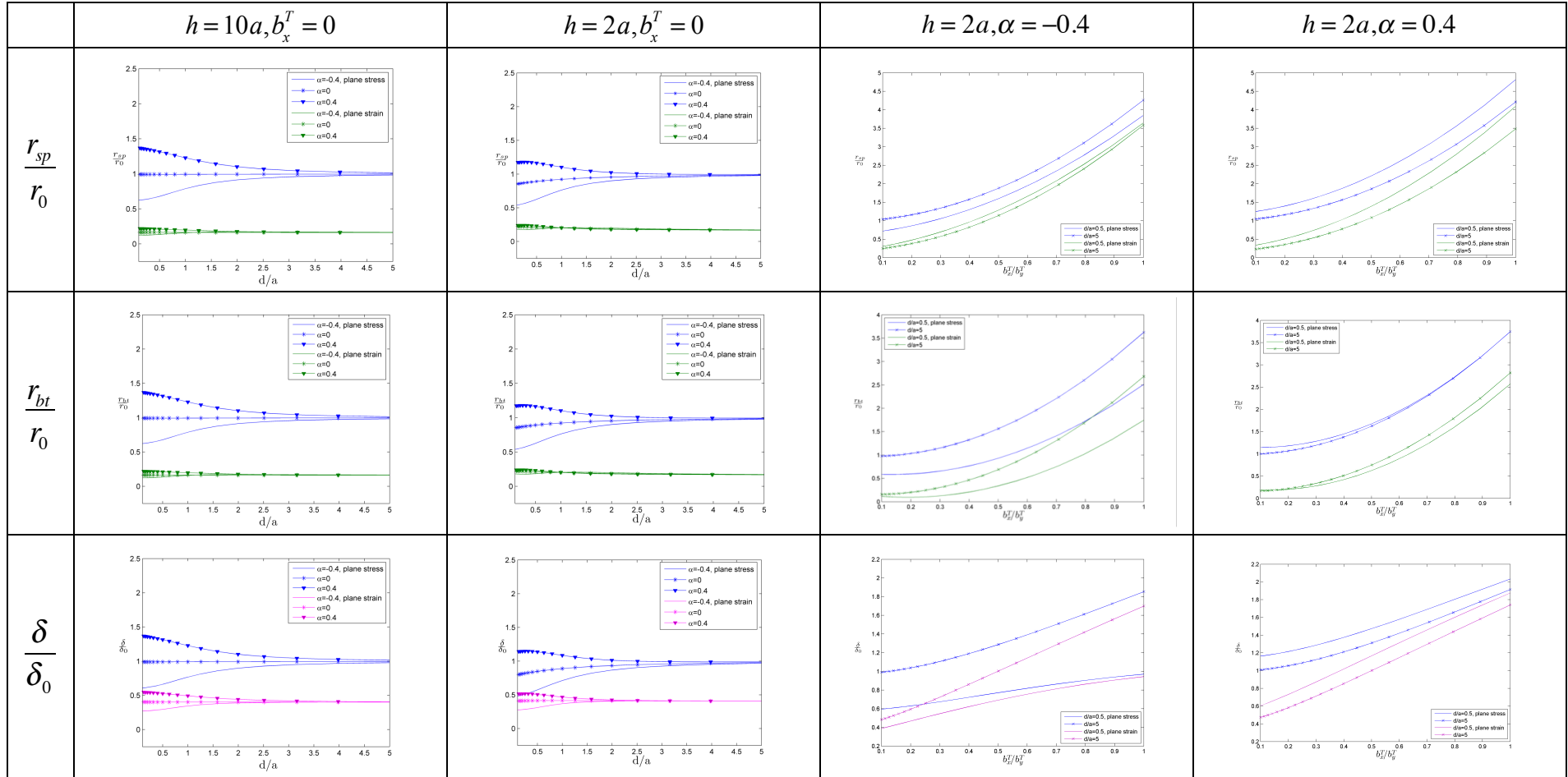
In Table 1, normalized PZS at the sharp (r_{sp}/r_0) and blunt tip (r_{bt}/r_0), and normalized CTOD (δ/δ_0) at the sharp tip of the Zener crack are depicted in different scenarios. For the case of $b_x^T = 0$, we may find the same α leads to a pair of identical plastic zones around two tips. In the most special situation $\alpha = 0$, if coating thickness h is very large compared to half-crack length a ($h = 10a$), it is verified from second column that values of r_p and δ converge to their corresponding values r_0 and δ_0 (they are called “reference values” in the context), no matter how far the crack is located beneath the interface.

Comparing figures in second and third columns, we observe that with a decreasing coating thickness, PZS at both tips, and CTOD at the sharp tip will be decreased. And the trend becomes more significant in plane stress than plane strain condition. This observation tells us a fact that increasing the volume fraction of added material (the coating) will enhance the ductility of the original structure (the substrate) in manner of magnifying the plastic deformation region around the crack tips.

Effects of the crack depth d can be viewed from third column ($h = 2a$), where different material mismatches have different reactions from a decreased crack depth. Softer coatings ($\alpha < 0$) shrink PZS and CTOD values lower than the reference while stiffer coatings ($\alpha > 0$) result in higher-than-reference plasticity quantities. This indicates a fact that when the crack gets nearer to the interface, it becomes easier to propagate with a softer coating covered on top, but stabilized under the protection of a stiffer coating.

Last two columns show continuous influence of displacement loads ratio b_x^T/b_y^T onto PZS and CTOD. Supposing that crack depth d can be either $0.5a$ or $5a$. If $x-dir$ displacement load gradually increases from $0.1 \times b_y^T$ to b_y^T , normalized r_p and δ will be increased without exceptions. As long as the crack is far away from the interface (for example $d/a = 5$), crack tip parameters become converge even within different material mismatches. But when the crack locates nearer, a thorough examination at different material mismatches tells that: a larger α always results in higher sensitivities of normalized r_p and δ along with the changing b_x^T/b_y^T . Besides, this effect onto plane strain cases is more significant than it does on plane stress cases.

Table 1. Normalized PZS and normalized CTOD, with $\beta = 0$



The effective stress intensity factors K_I^{eff} and K_{II}^{eff}

Due to the inclusion of the 1st order plastic zone size, we can see from Table 2, generally speaking, K_I^{eff}/K_I and K_{II}^{eff}/K_{II} are lower than 1. However the scale of decrement depends on material mismatches, crack depths and many more. One can see that K_I^{eff}/K_I and K_{II}^{eff}/K_{II} deduce more when the coating is stiffer ($\alpha > 0$), meaning that the correction of K_I and K_{II} is more necessary if the substrate is coated with stiffer material.

Moreover, when $\alpha < 0$, crack with greater depth shows smaller values of K_I^{eff}/K_I and K_{II}^{eff}/K_{II} . Similar trends can be seen when $\alpha > 0$ and crack gets closer to the interface. This illustrates that cases of shallower crack under stiffer coating, or deeper crack under softer coating, are in greater need of correction in terms of stress intensity factors. It is also not difficult to find K_I^{eff} and K_{II}^{eff} of the sharp tip of a Zener crack under plane stress differ more from K_I and K_{II} respectively than the results shown for plane strain condition.

Table 2. Effective stress intensity factors K_I^{eff} and K_{II}^{eff} , with $\beta = 0$, $h = 2a$, $b_x^T/b_y^T = 0.5$

d/a		0.1	0.2	0.3	0.4	0.5	0.6
$\alpha = -0.4$	$\frac{K_I^{eff}}{K_I}$ Plane stress	0.99827	0.99822	0.99818	0.99815	0.99812	0.99808
	K_I Plane strain	0.99857	0.99853	0.99851	0.99850	0.99848	0.99847
	$\frac{K_{II}^{eff}}{K_{II}}$ Plane stress	0.99783	0.99777	0.99772	0.99767	0.99763	0.99758
	K_{II} Plane strain	0.99820	0.99816	0.99813	0.99811	0.99809	0.99807
$\alpha = 0.4$	$\frac{K_I^{eff}}{K_I}$ Plane stress	0.99682	0.99694	0.99704	0.99713	0.99720	0.99727
	K_I Plane strain	0.99791	0.99802	0.99810	0.99818	0.99824	0.99830
	$\frac{K_{II}^{eff}}{K_{II}}$ Plane stress	0.99625	0.99631	0.99637	0.99642	0.99648	0.99653
	K_{II} Plane strain	0.99753	0.99761	0.99767	0.99773	0.99779	0.99784

Conclusions

In the present work, plastic zone size, crack tip opening displacement and effective stress intensity factors for a sub-interface Zener-Stroh crack in a coating-substrate system under combined displacement load $b^T = b_y^T + ib_x^T$ are investigated by a generalized Irwin model. In the numerical examples, we specifically describe the dependence of normalized plastic zone size for sharp tip r_{sp}/r_0 , for blunt tip r_{bt}/r_0 , normalized crack tip opening displacement for sharp tip δ/δ_0 , as well as normalized effective stress intensity factors for sharp tip K_I^{eff}/K_I , K_{II}^{eff}/K_{II} on normalized crack depth d/a , normalized coating thickness h/a , Dundurs' parameter α , and displacement loads ratio b_x^T/b_y^T . According to the results obtained and discussed, following conclusions can be made:

1. Either the Zener-Stroh crack exists in an infinite bi-material composite without mismatches ($\alpha = \beta = 0$), or it locates far from the interface ($d/a > 5$)

- in a coating-substrate system with mismatches (arbitrary α and β), the current physical problem reduces to the corresponding problem of the same crack in a homogeneous material.
2. Normalized PZS and normalized CTOD will be increased with the increasing coating thickness. When coating thickness is fixed, a Zener crack moves nearer to the interface will experience higher PZS and CTOD values if the substrate is coated with stiffer material, but lower PZS and CTOD if it has a softer coating instead.
 3. These are the circumstances shall we need to produce the effective stress intensity factors: 1) if the coating is softer than the substrate and the crack is relatively deep beneath the interface; 2) if the coating is stiffer than the substrate and the crack locates near the interface; 3) choose substrate with stiffer-coating system to evaluate when the other conditions are the same; 4) choose plane stress structure to evaluate when the other conditions are the same.
 4. When the coating thickness and crack depth are fixed, with the increasing displacement loads ratio b_x^T / b_y^T , normalized PZS and normalized CTOD grows more rapidly and around higher values if the substrate is coated with stiffer materials, especially in plane strain condition.

Reference

- Anderson, T. L. (2005). *Fracture Mechanics: Fundamentals and Applications*: Taylor & Francis.
- Koch, C. C. (2007). Structural nanocrystalline materials: an overview. *Journal of materials science*, 42(5), 1403-1414.
- Kumar, K., Van Swygenhoven, H., & Suresh, S. (2003). Mechanical behavior of nanocrystalline metals and alloys. *Acta Materialia*, 51(19), 5743-5774.
- Kuntz, J. D., Zhan, G.-D., & Mukherjee, A. K. (2004). Nanocrystalline-matrix ceramic composites for improved fracture toughness. *Mrs Bulletin*, 29(01), 22-27.
- Lu, H., & Lardner, T. J. (1992). Mechanics of Subinterface Cracks in Layered Material. *International Journal of Solids and Structures*, 29(6), 669-688.
- Pozdnyakov, V. (2003). Nanostructural crack arrest. *Technical Physics Letters*, 29(2), 151-153.
- Stroh, A. N. (1954). The formation of cracks as a result of plastic flow. *Proc. Roy. Soc. London*, 223A, 404-414.
- Wang, Y., Chen, M., Zhou, F., & Ma, E. (2002). High tensile ductility in a nanostructured metal. *Nature*, 419(6910), 912-915.
- Weertman, J. (1996). *Dislocation Based Fracture Mechanics*: World Scientific.
- Zener, C. (1948). *The micro-mechanism of fracture*. Paper presented at the Fracturing of Metals, Cleveland.
- Zhang, S., Sun, D., Fu, Y., & Du, H. (2005). Toughening of hard nanostructural thin films: a critical review. *Surface and Coatings Technology*, 198(1), 2-8.
- Zhao, Y.-H., Liao, X.-Z., Cheng, S., Ma, E., & Zhu, Y. T. (2006). Simultaneously increasing the ductility and strength of nanostructured alloys. *Advanced Materials*, 18(17), 2280-2283.
- Zhuang, J., Yi, D. K., & Xiao, Z. M. (2013). Elastic-plastic analysis of a sub-interface crack in a coating-substrate composite. *International Journal of Solids and Structures*, 50(2), 414-422. doi: <http://dx.doi.org/10.1016/j.ijsolstr.2012.10.018>